HHS Public Access

Author manuscript

J Thorac Oncol. Author manuscript; available in PMC 2021 January 15.

Published in final edited form as:

J Thorac Oncol. 2018 August ; 13(8): 1121–1127. doi:10.1016/j.jtho.2018.04.027.

Radiosensitivity of lung metastases by primary histology and implications for stereotactic body radiation therapy using the genomically adjusted radiation dose

Kamran A. Ahmed, MD[1], **Jacob G. Scott, MD**[2], **John A. Arrington, MD**[3], **Arash O. Naghavi, MD**[1], **G. Daniel Grass, MD PhD**[1], **Bradford A. Perez, MD**[1], **Jimmy J. Caudell, MD PhD**[1], **Anders E. Berglund, PhD**[4], **Eric A. Welsh, PhD**[4], **Steven A. Eschrich, PhD**[4], **Thomas J. Dilling, MD**[1,*], **Javier F. Torres-Roca, MD**[1,*]

[1]Department of Radiation Oncology, H. Lee Moffitt Cancer Center and Research Institute, Tampa, FL 33612, USA

[2]Cleveland Clinic Department of Radiation Oncology, Cleveland, OH 44195

[3]Department of Radiology, H. Lee Moffitt Cancer Center and Research Institute, Tampa, FL 33612, USA

[4]Department of Bioinformatics H. Lee Moffitt Cancer Center and Research Institute, Tampa, FL 33612, USA

Abstract

Introduction: We assessed the radiosensitivity of lung metastases based on primary histology using a validated gene signature and model lung metastases for the genomically adjusted radiation dose (GARD).

Methods: Tissue samples were identified from our prospective observational protocol. The radiosensitivity index (RSI) 10 gene assay was run on samples and calculated alongside GARD using the previously published algorithms. A cohort of 105 patients with 137 lung metastases treated with SBRT at our institution was used for clinical correlation.

Results: A total of 138 unique metastatic lung lesions were identified for inclusion from our institution's tissue biorepository. There were significant differences in the RSI of lung metastases based on histology. In order of decreasing radioresistance, the median RSIs were endometrial adenocarcinoma (0.49), soft tissue sarcoma (0.47), melanoma (0.44), rectal adenocarcinoma (0.43), renal cell carcinoma (0.33), head and neck squamous cell cancer (0.33), colon adenocarcinoma (0.32), and breast adenocarcinoma (0.29), p=0.002. We modeled GARD for these

[*]**Corresponding Authors:** Thomas J. Dilling MD and Javier F. Torres-Roca MD, H. Lee Moffitt Cancer Center and Research Institute, Department of Radiation Oncology, 12902 Magnolia Dr., Tampa, FL 33612 USA, Telephone: 00-1-813-745-3565, Fax: 00-1-813-745-7231, thomas.dilling@moffitt.org and javier.torresroca@moffitt.org.

Conflicts of Interest: Steven A. Eschrich PhD and Javier F. Torres-Roca MD report stock and leadership in Cvergenx, Inc. and royalty and patents on RSI. All remaining authors have declared no conflicts of interest.

samples and identified the BED necessary to optimize local control. The 12 and 24 month Kaplan-Meier rates of local control for radioresistant vs radiosensitive histologies from our clinical correlation cohort following lung SBRT were 92%/87% and 100%, respectively (p=0.02).

Conclusions: In this analysis, we note significant differences in radiosensitivity based on primary histology of lung metastases and model the BED necessary to optimize local control. This study suggests primary histology may be an additional factor to consider in lung SBRT dose selection and dose personalization may be feasible.

Keywords

Radiosensitivity index; lung metastases; radiation sensitivity; genomically adjusted radiation dose

Introduction

The management of oligometastatic disease has become increasingly common among radiation oncologists[1]. One of the primary sites in which radiation therapy is utilized in this setting is for the management of lung metastases. Stereotactic body radiation therapy (SBRT) is an excellent treatment approach with control rates of > 90% reported in both prospective and retrospective series[2–4].

Several studies have discussed the role primary histology may have in local control outcomes following SBRT for lung metastases[4–7]. Reports have suggested colorectal metastases may be more prone to local recurrence[4] while others have suggested rectal cancer may be more likely to locally recur than colon primaries[5]. The radiosensitivity index (RSI) is a previously developed and extensively validated gene signature for assessment of the inherent radiosensitivity/radioresistance of tumors[8–12]. Our group previously reported on the use of RSI on metastatic disease in the setting of colon primaries and metastases[13] according to anatomical location as well as brain[14] and liver metastases[15] according to primary histology. When assessing liver metastases, we noted differences in the RSI of surgically resected samples correlated with local control rates following 5 fraction SBRT at our institution[15]. We noted RSI-determined radioresistant histologies such as colorectal fared worse in local control compared to more radiosensitive histologies such as breast, lung and anal cancers.

We have previously developed the genomically adjusted radiation dose (GARD) as a method of radiation dose personalization[16]. Significant differences were noted in the modeled GARD between clinically radiosensitive tumors including cervical and oropharyngeal cancers compared to clinically radioresistant tumors such as glioblastoma and sarcoma. GARD predicted clinical outcomes in five independent datasets and has been noted to be the first personalized approach to radiation delivery and a priority for clinical trial application[17, 18]. In this manuscript, we undertook an analysis of the RSI of lung metastases in our center's tissue biorepository and propose a model for dose personalization using GARD identifying tissue samples likely to benefit from dose escalation beyond a 100 Gy BED. These results were correlated to an independent dataset of patients treated with lung SBRT at our institution.

Patients and Methods

Patients were identified from the IRB-approved Total Cancer Care (TCC) prospective observational protocol at Moffitt Cancer Center[19]. Data from a total of 138 unique metastatic lung lesions were obtained from the TCC data pool for patients treated at Moffitt Cancer Center.

RNA Preparation and Gene Expression Profiling

These methods have been described previously[16]. Briefly, gene expression values for the samples in this study were extracted from the TCC database. These expression values were normalized against a median sample using the previously reported iterative rank order normalization method[20]. An RNA-quality related batch-effect was identified in the resulting normalized data, which was removed by training a partial least squares (PLS) model[21] to the RNA integrity number (RIN), and then subtracting the first partial least squares component.

Radiosensitivity Signature

The previously tested 10 gene assay was run on tissue samples ranked according to gene expression. RSI was calculated using the previously published ranked based algorithm[8, 9]. Each of the 10 genes in the assay was ranked according to gene expression [from the highest (10) to the lowest expressed gene (1)]. RSI was determined using the previously published ranked based linear algorithm:

$$\begin{aligned}\mathrm{RSI} = {} & -0.0098009 * \mathrm{AR} + 0.0128283 * \mathrm{cJun} + \\ & 0.0254552 * \mathrm{STAT1} - 0.0017589 * \mathrm{PKC} - \\ & 0.0038171 * \mathrm{RelA} + 0.1070213 * \mathrm{cABL} - \\ & 0.0002509 * \mathrm{SUMO1} - 0.0092431 * \mathrm{PAK2} - \\ & 0.0204469 * \mathrm{HDAC1} - 0.0441683 * \mathrm{IRF1}\end{aligned}$$

Genomically Adjusted Radiation Dose

The formulation of GARD has been previously described[16]. GARD scores were derived using the linear quadratic model and the individual gene-expression-based RSI. We calculated GARD using a script written into Excel. The final GARD formula is GARD=nd($\alpha + \beta$d). GARD was modeled for a dose of 84 Gy in 2 Gy fractions, the equivalent dose at 2 Gy (EQD2) of 10 Gy X 5 fractions using a α/β of 10. An 8.4% failure rate was assumed with 100 BED[22]. The calculation for GARD is similar to the biologically effective dose, except the patient-specific α is derived by substituting the radiosensitivity index for survival (S) in $S = e^{-nd(\alpha + \beta d)}$, where dose (d) is 2 Gy, n=1, and β is a constant (0.05/Gy)[23]. A higher GARD value predicts a higher radiation therapeutic effect.

Lung SBRT Cohort

Using our institutional database of patients treated with SBRT to the lung, a retrospective analysis was conducted on all consecutive patients treated for lung metastases with a dose of 50 Gy in 5 fractions or 60 Gy in 5 or 8 daily fractions. Each patient was immobilized using the Body-Fix thoracic-T double vacuum immobilization system (Medical Intelligence, Schwabmünchen, Germany). Axial CT images were obtained on a 16-slice CT simulator (GE HealthCare, Milwaukee, WI) with 3 mm thickness image acquisition. Four-dimensional

CT imaging was performed using Varian RPM (Varian, Palo Alto, CA). In some cases, respiratory gating was employed, using an infrared reflector placed on the patient's chest. Prior to each treatment, an initial cone-beam computed tomography (CBCT) scan was acquired, a match was performed, and the shift was applied. Any shift greater than 0.3 cm required a second CBCT acquisition to verify position. The planning target volume (PTV) equaled the gross tumor volume (GTV) plus 7 mm superiorly and inferiorly and 5 mm radially. The PTV was covered by 95% of the prescribed dose. Dose constraints included the spinal cord 0.03 cc <17 Gy, lung V20 <10%, mean lung dose < 600 cGy, esophagus V27.5 < 5 cc, chestwall V30 <30 cc, heart mean <10 Gy, heart V32 <15 cc, and brachial plexus V30 <3 cc.

Following treatment, lesions were followed by the treating radiation oncologist or medical oncologist with imaging at 2–3 month intervals. Radiologic imaging was reviewed to determine local control. An independent review of imaging to assess local control was undertaken by a radiation oncologist (KAA) and a radiologist (JAA). Local failure was defined by an increase in the size of the previously irradiated area according to the RECIST criteria version 1.1[24] and distinguished from post-radiation change by continued growth of tumor on subsequent imaging. Direct RSI measurements for this cohort were not performed due to tissue unavailability. To classify each histology as either radiosensitive or radioresistant, we utilized the median RSI observed in the genomically-profiled tissue institutional biorepository. Using a previously reported median RSI cutpoint (RSI ≥0.375 = radioresistant)[13] RSI-determined radioresistant histologies included soft tissue sarcoma (n=29; 21%), melanoma (n=25; 18%), and rectal adenocarcinoma (n=17; 12%). In contrast, RSI-radiosensitive histologies included renal cell carcinoma (n=15; 11%), head and neck squamous cell cancer (n=7; 5%), colon adenocarcinoma (n=36; 26%), and breast adenocarcinoma (n=8; 6%).

Statistical Analysis

Descriptive statistics were used to summarize the cohort including median and range for continuous variables or counts and percentages for categorical variables. When comparing RSI values between groups, the Kruskal–Wallis test was used. To test differences between cohorts, the Wilcoxon, Pearson's chi-square and Fisher's exact tests were used when appropriate. Overall survival and local control rates were calculated from the last day of treatment to the date of death or progression using the Kaplan–Meier (KM) method. Cox proportional hazard model analyses were performed. A two-tailed $p<0.05$ was considered statistically significant. Statistical analyses were performed using JMP 13 (SAS Institute Inc, Cary, NC, USA). Box plots were generated using MATLAB (version R2013a Natick, Massachusetts: The MathWorks Inc., 2010).

Results

The RSI of Lung Metastases

A total of 138 samples from 126 patients were identified from our prospective tissue collection cohort. The most common histologies were colon adenocarcinoma (n=38; 28%),

melanoma (n=33; 24%), and soft tissue sarcoma (n=29; 21%). The median RSI for all lung metastases was 0.42 (Q1 0.31; Q3 0.49).

Significant differences were noted in the RSI of lung metastases based upon primary histology. In order of decreasing radioresistance, the median RSIs were endometrial adenocarcinoma (0.49), soft tissue sarcoma (0.47), melanoma (0.44), rectal adenocarcinoma (0.43), head and neck squamous cell cancer (0.33), renal cell carcinoma (0.33), colon adenocarcinoma (0.32), and breast adenocarcinoma (0.29), p=0.002. A box plot showing RSI values according to primary histology is shown in Figure 1.

GARD Modeling

Modeling GARD for a total delivered dose of 84 Gy in 2 fractions, the EQD2 equivalent of the 100 BED, 10 Gy X 5 SBRT fractionation, we noted a large heterogeneity in GARD values across histologies. The median delivered GARD in increasing order was endometrial adenocarcinoma (29.8), soft tissue sarcoma (31.7), melanoma (34.7), rectal adenocarcinoma (35.2), head and neck SCC (46.7), renal cell carcinoma (47.2), colon adenocarcinoma (47.7), and breast adenocarcinoma (51.5) p=0.002. When modeling an 8.4% failure rate, we identified 11 lesions in our dataset at risk for local failure. These lesions received a median GARD of 17.5 (range: 8.5–24.8) and are identified inferior to the red line in Figure 2. These lesions all had an RSI ≥ 0.55 and were of sarcoma and melanoma primary histology.

Figure 3 details the BED for 2 Gy fractions required for lesions to achieve a GARD ≥ 25.1, the minimum GARD required for local control predicted by our model. Interestingly, a sigmoidal relationship is observed where the largest influence of dose occurs in the range of 50 to 100 BED. In this BED range, 22% to 90% of patient's achieve an optimized GARD. However, between 100 to 200 BED only an additional 7% of patient's achieve an optimized GARD.

Clinical Outcomes Following Lung SBRT

A total of 105 patients treated to 137 metastatic lung lesions with SBRT were identified at our institution for clinical correlation. Patients were treated between August 2007 and March 2017. A total of 66 (48%) lesions were from histologies identified as RSI-determined radiosensitive in our biorepository and 71 (52%) from RSI-determined radioresistant histologies. Median follow-up for lesions was 16 months (range: 1.2–88.9 months). Clinical characteristics for the two cohorts are detailed in Table 1. There was no difference in the two groups in terms of age (p=0.14), gender (p=0.13), the maximum diameter of the metastases (p=0.2), number of lines of previous systemic therapy prior to SBRT (p=0.97) or SBRT dose (p=0.18).

Five local failure events were noted for an overall 12/24 month KM local control rate of 96%/93%. All local failures occurred in RSI-determined radioresistant histologies. These included two sarcoma lesions, 2 rectal lesions, and 1 melanoma. One rectal lesion was treated to 60 Gy in 8 fractions and one sarcoma lesion treated to 50 Gy in 5 fractions, the three others were treated to 60 Gy in 5 fractions. Characteristics of these 5 cases of local failure are detailed in Table 2. Significant differences in local control were noted between radioresistant and radiosensitive histologies. The 12 and 24 month KM local control rates

were 92%/87% and 100%, respectively (p=0.02), Figure 4. Other factors such as dose 60 Gy/5 vs others (p=0.39) and size ≥1.5 cm vs <1.5 cm (p=0.66) were not found to predict for local control on univariate analysis.

Overall survival in the cohort at 12 and 24 months was 90% and 72%, respectively. No differences were noted in overall survival between the radioresistant and radiosensitive cohorts 90%/71% and 91%/72% (p=0.68) at 12/24 months, respectively.

Discussion

In this manuscript, we detail the genomic profiling results of lung metastases based on RSI. We note significant differences of lung metastases based on primary histology. Radioresistant histologies identified by RSI were noted to include endometrial adenocarcinoma, soft tissue sarcoma, melanoma, and rectal adenocarcinoma whereas renal cell carcinoma, head and neck squamous cell cancer, colon adenocarcinoma, and breast adenocarcinoma were noted to be (comparatively) radiosensitive. Modeling GARD for an EQD2 of 10 Gy X 5, we identify lesions at risk of local failure and candidates for potential dose optimization in future personalized SBRT dosing trials. These results were similar to results in our independent institutional cohort of metastatic lung lesions treated with lung SBRT.

Several studies have reported on the impact histology can have in the outcome of SBRT treated lung metastases. These include studies revealing colorectal metastases may fare worse following lung SBRT treatment than other histologies. A study from Binkley et al reported colorectal metastases had a significantly higher cumulative incidence of local failure compared to other histologies with 24 month local failure rates of 42% vs. 9% p<0.0004[4]. However, this lower local control for colorectal metastases may be due to rectal lesions faring worse than those of colon. A study from Kinj et al revealed there was a significant difference in the local control of colon metastases vs. those of rectal metastases[5] following lung SBRT. The study suggested one of the reasons for this difference may be an inherent radioresistance in rectal tumors due to the routine use of neoadjuvant radiation in primary management of the disease and recurrent cells arising from radioresistant clones as well as a higher rate of KRAS mutations in rectal lesions. Similar results have been noted by de Baere et al with rectal metastases faring worse in local control compared to colon following radiofrequency ablation of lung metastases[25]. Our local control outcomes also support the findings of these two studies. We noted two local failures in rectal lesions but none in colon. Although differences in local control were noted in our series by primary histology, the overall local control rate is high as reported by other institutions[1]. Furthermore, we noted a separation of colon and renal lung samples into both radioresistant and radiosensitive populations based on RSI, a finding that could be explored in future analyses.

Various dose and fractionation schedules for lung SBRT have been studied in the retrospective and prospective settings. The only study to assess the effect of two SBRT schedules in the prospective setting for primary non-small cell lung cancer has been RTOG 0915[26]. No differences in tumor control were noted between 34 Gy in 1 fraction and 48 Gy

in 4 fractions[27]. The ongoing TROG 13.01 SAFFRON II study is assessing 28 Gy in 1 fraction vs. 48 Gy in 4 fractions in pulmonary oligometastases[28]. However, the BEDs of these two fractionation schemes are very similar, 106.4 and 105.6, respectively. With high rates of local control, decreasing toxicity and treatment burden is the primary goal of the TROG 13.01 study. The optimal SBRT dose and fractionation for lung metastases remains an open question.

Onishi et al noted an 8.4% failure rate following a delivered dose of 100 Gy BED[22]. We modeled the expected distribution of GARD values achieved with uniform 100 Gy BED and identify significant heterogeneity achieved in GARD values in spite of uniform physical dose. Our model proposes that patients with a GARD value below 25.1 are at higher risk for recurrence. A total of 11 lesions in our cohort would have met this criterion. These lesions have an RSI of ≥ 0.55 and represent a cohort of patients that may benefit from genomically guided dose optimization beyond 100 BED. These 11 lesions were of primary melanoma and sarcoma histology. Similarly, we noted three of the 5 failures in our clinical cohort to be of melanoma and sarcoma primary histology. Finally, we model the BED in 2 Gy equivalent fractions required to achieve a GARD ≥ 25.1, the minimum GARD to achieve local control as predicted by our model. The sigmoidal shape of the curve indicates the greatest influence of dose occurs in the range of 50 to 100 BED, while 3% of lesions (n=4) continue to be at risk of local failure past 200 BED. We hypothesize GARD can be applied as a method of dose personalization in the setting of SBRT to lung metastases.

Although, the current analysis offers a novel approach to personalization of lung SBRT dose, the study is not without limitations. The primary limitation of this analysis is that RSI values are not available for our clinical correlation cohort of lesions treated with SBRT. RSI was run on resected surgical tissue from our institution's biorepository and this tissue was used as a model to determine the impact of primary histology on RSI. In addition, there are a few disease sites (breast, HNSCC, and endometrial) in which there are limited RSI samples (<5) which limits the ability to draw conclusions for these tumors. However, our results utilize the previously validated GARD metric for radiation dose personalization and support the impact primary histology has on local control following lung SBRT.

In this study, we note significant differences in lung metastases based on primary histology. We also propose a method of personalization to tailor radiation dose to the genomic profile of lung metastases. As we move closer to an era where personalization of radiation dose to an individual tumor may be a reality, practitioners may pay closer attention to primary histology in the management of oligometastatic disease.

Acknowledgements:

The study was supported in part under the Merck-Moffitt Cancer Center Research Collaboration.

Funding: This work was supported by National Institutes of Health [grant numbers R21CA101355, R21CA135620]; US Army Medical Research and Materiel Command; National Functional Genomics Center Award [grant number 170220051]; Bankhead-Coley Foundation Award [grant number 09BB-22]; and the Debartolo Family Personalized Medicine Institute.

References

1. Ahmed KA, Torres-Roca JF. Stereotactic Body Radiotherapy in the Management of Oligometastatic Disease. Cancer control : journal of the Moffitt Cancer Center 2016;23:21–29. [PubMed: 27009453]
2. Milano MT, Katz AW, Zhang H, et al. Oligometastases treated with stereotactic body radiotherapy: long-term follow-up of prospective study. International journal of radiation oncology, biology, physics 2012;83:878–886.
3. Salama JK, Hasselle MD, Chmura SJ, et al. Stereotactic body radiotherapy for multisite extracranial oligometastases: final report of a dose escalation trial in patients with 1 to 5 sites of metastatic disease. Cancer 2012;118:2962–2970. [PubMed: 22020702]
4. Binkley MS, Trakul N, Jacobs LR, et al. Colorectal Histology Is Associated With an Increased Risk of Local Failure in Lung Metastases Treated With Stereotactic Ablative Radiation Therapy. International journal of radiation oncology, biology, physics 2015;92:1044–1052.
5. Kinj R, Bondiau PY, Francois E, et al. Radiosensitivity of Colon and Rectal Lung Oligometastasis Treated With Stereotactic Ablative Radiotherapy. Clinical colorectal cancer 2017;16:e211–e220. [PubMed: 27670890]
6. Qiu H, Katz AW, Chowdhry AK, et al. Stereotactic Body Radiotherapy for Lung Metastases from Colorectal Cancer: Prognostic Factors for Disease Control and Survival. American journal of clinical oncology 2015.
7. Takeda A, Kunieda E, Ohashi T, et al. Stereotactic body radiotherapy (SBRT) for oligometastatic lung tumors from colorectal cancer and other primary cancers in comparison with primary lung cancer. Radiotherapy and oncology : journal of the European Society for Therapeutic Radiology and Oncology 2011;101:255–259. [PubMed: 21641064]
8. Eschrich S, Zhang H, Zhao H, et al. Systems biology modeling of the radiation sensitivity network: a biomarker discovery platform. International journal of radiation oncology, biology, physics 2009;75:497–505.
9. Eschrich SA, Pramana J, Zhang H, et al. A gene expression model of intrinsic tumor radiosensitivity: prediction of response and prognosis after chemoradiation. International journal of radiation oncology, biology, physics 2009;75:489–496.
10. Eschrich SA, Fulp WJ, Pawitan Y, et al. Validation of a radiosensitivity molecular signature in breast cancer. Clinical cancer research : an official journal of the American Association for Cancer Research 2012;18:5134–5143. [PubMed: 22832933]
11. Torres-Roca JF, Fulp WJ, Caudell JJ, et al. Integration of a Radiosensitivity Molecular Signature Into the Assessment of Local Recurrence Risk in Breast Cancer. International journal of radiation oncology, biology, physics 2015;93:631–638.
12. Ahmed KA, Chinnaiyan P, Fulp WJ, et al. The radiosensitivity index predicts for overall survival in glioblastoma. Oncotarget 2015;6:34414–34422. [PubMed: 26451615]
13. Ahmed KA, Fulp WJ, Berglund AE, et al. Differences Between Colon Cancer Primaries and Metastases Using a Molecular Assay for Tumor Radiation Sensitivity Suggest Implications for Potential Oligometastatic SBRT Patient Selection. International journal of radiation oncology, biology, physics 2015;92:837–842.
14. Ahmed KA, Berglund AE, Welsh EA, et al. The radiosensitivity of brain metastases based upon primary histology utilizing a multigene index of tumor radiosensitivity. Neuro-oncology 2017;19:1145–1146. [PubMed: 28379582]
15. Ahmed KA, Caudell JJ, El-Haddad G, et al. Radiosensitivity Differences Between Liver Metastases Based on Primary Histology Suggest Implications for Clinical Outcomes After Stereotactic Body Radiation Therapy. International journal of radiation oncology, biology, physics 2016;95:1399–1404.
16. Scott JG, Berglund A, Schell MJ, et al. A genome-based model for adjusting radiotherapy dose (GARD): a retrospective, cohort-based study. The Lancet Oncology 2017;18:202–211. [PubMed: 27993569]
17. Jaffee EM, Dang CV, Agus DB, et al. Future cancer research priorities in the USA: a Lancet Oncology Commission. The Lancet Oncology 2017;18:e653–e706. [PubMed: 29208398]

18. Poortmans P, Kaidar-Person O, Span P. Radiation oncology enters the era of individualised medicine. The Lancet Oncology 2017;18:159–160. [PubMed: 27993570]
19. Fenstermacher DA, Wenham RM, Rollison DE, et al. Implementing personalized medicine in a cancer center. Cancer journal 2011;17:528–536.
20. Welsh EA, Eschrich SA, Berglund AE, et al. Iterative rank-order normalization of gene expression microarray data. BMC bioinformatics 2013;14:153. [PubMed: 23647742]
21. Wold SRA, Wold H, Dunn I, WJ. . The collinearity problem in linear regression. The partial least squares (PLS) approach to generalized inverses. . SIAM Journal on Scientific and Statistical Computing 1984;5:735–743.
22. Onishi H, Shirato H, Nagata Y, et al. Hypofractionated stereotactic radiotherapy (HypoFXSRT) for stage I non-small cell lung cancer: updated results of 257 patients in a Japanese multi-institutional study. Journal of thoracic oncology : official publication of the International Association for the Study of Lung Cancer 2007;2:S94–100.
23. Jeong J, Shoghi KI, Deasy JO. Modelling the interplay between hypoxia and proliferation in radiotherapy tumour response. Phys Med Biol 2013;58:4897–4919. [PubMed: 23787766]
24. Eisenhauer EA, Therasse P, Bogaerts J, et al. New response evaluation criteria in solid tumours: revised RECIST guideline (version 1.1). European journal of cancer 2009;45:228–247. [PubMed: 19097774]
25. de Baere T, Auperin A, Deschamps F, et al. Radiofrequency ablation is a valid treatment option for lung metastases: experience in 566 patients with 1037 metastases. Annals of oncology : official journal of the European Society for Medical Oncology 2015;26:987–991. [PubMed: 25688058]
26. Siva S, Slotman BJ. Stereotactic Ablative Body Radiotherapy for Lung Metastases: Where is the Evidence and What are We Doing With It? Seminars in radiation oncology 2017;27:229–239. [PubMed: 28577830]
27. Videtic GM, Hu C, Singh AK, et al. A Randomized Phase 2 Study Comparing 2 Stereotactic Body Radiation Therapy Schedules for Medically Inoperable Patients With Stage I Peripheral Non-Small Cell Lung Cancer: NRG Oncology RTOG 0915 (NCCTG N0927). International journal of radiation oncology, biology, physics 2015;93:757–764.
28. Siva S, Kron T, Bressel M, et al. A randomised phase II trial of Stereotactic Ablative Fractionated radiotherapy versus Radiosurgery for Oligometastatic Neoplasia to the lung (TROG 13.01 SAFRON II). BMC cancer 2016;16:183. [PubMed: 26944262]

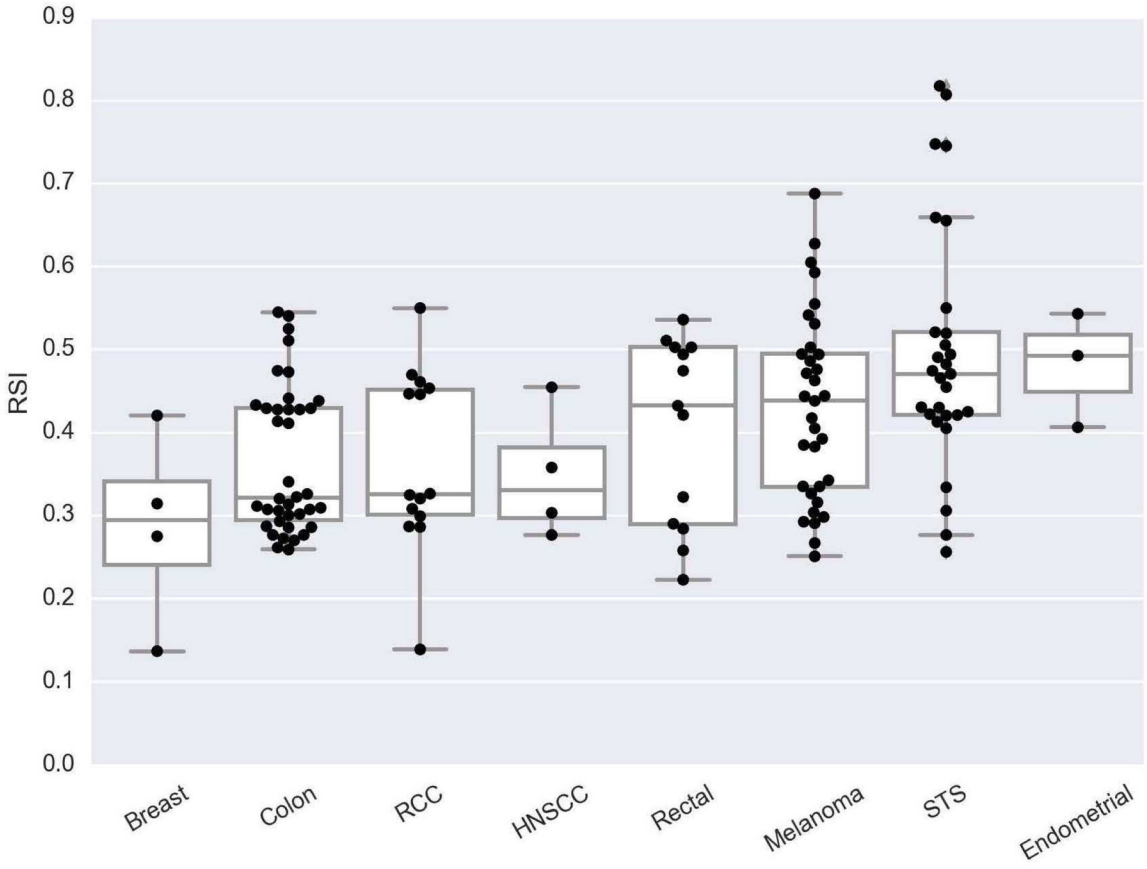

Figure 1:

Box plot of RSI differences among lung metastases based on primary histology, p=0.002. Abbreviations: RCC = Renal cell cancer, HNSCC = Head and neck squamous cell cancer, STS = Soft tissue sarcoma.

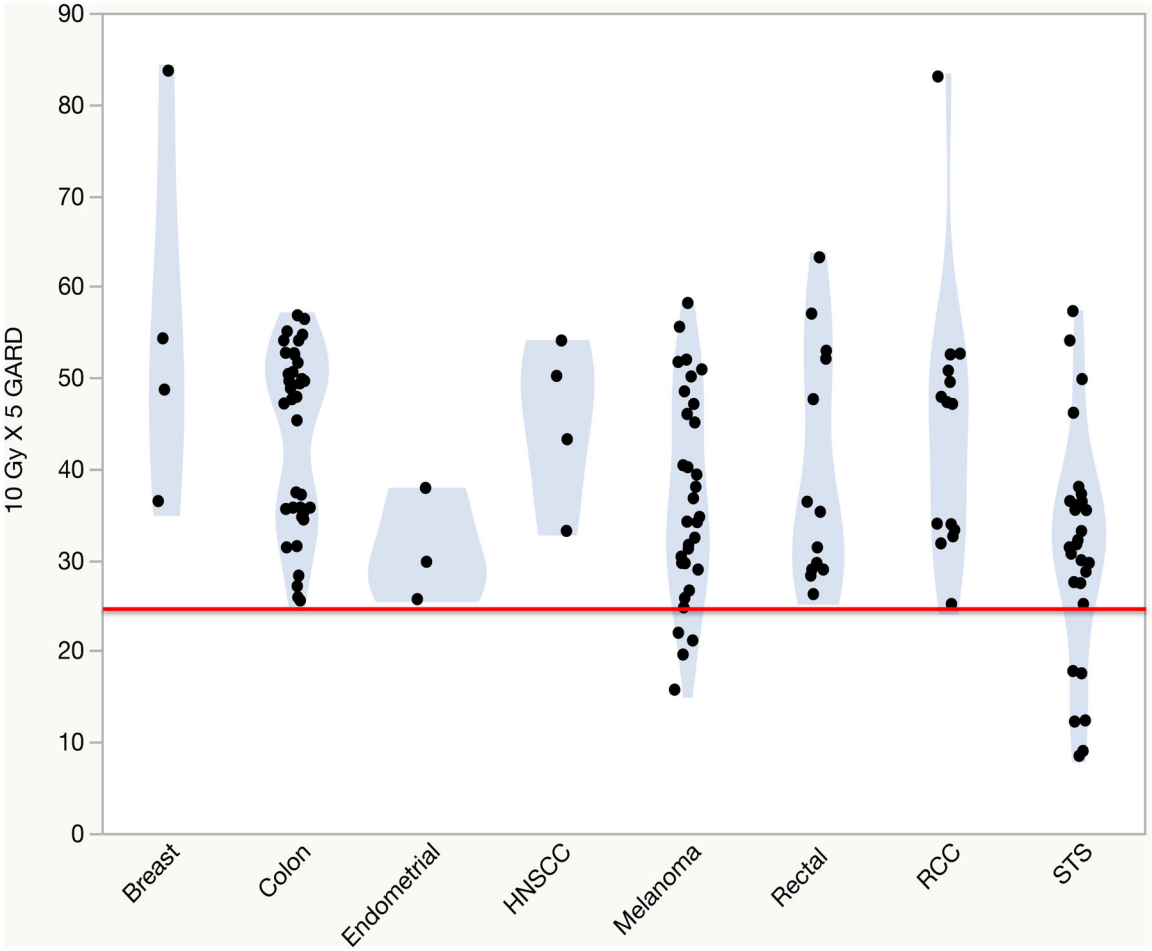

Figure 2:

A model of GARD values for an equivalent dose of 2 Gy (EQD2) of 10 Gy X 5 according to primary histology. The red line indicates an 8.4% failure rate. Abbreviations: RCC = Renal cell cancer, HNSCC = Head and neck squamous cell cancer, STS = Soft tissue sarcoma.

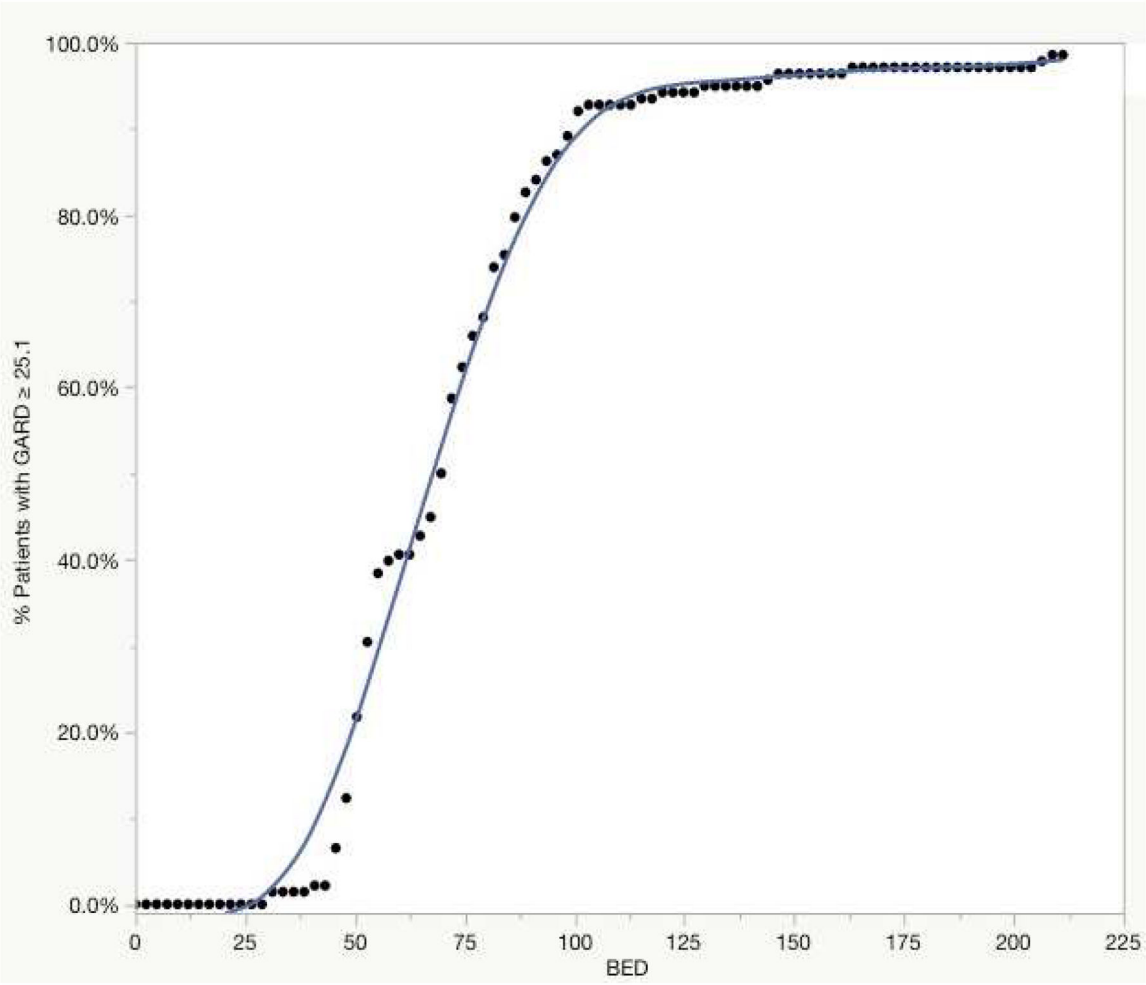

Figure 3:
A model for the percent of patients achieving a GARD ≥ 25.1 with 2 Gy biologic effective doses (BED).

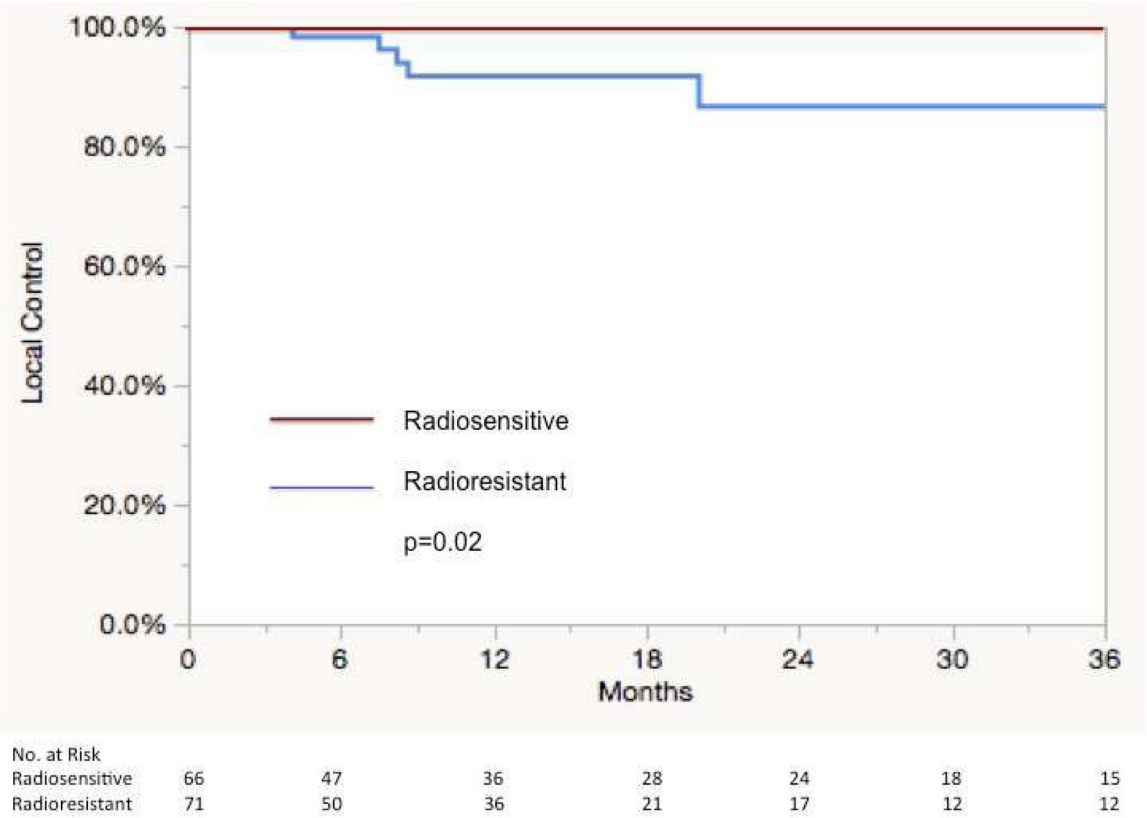

Figure 4:

Kaplan-Meier Curve of local control following SBRT according to radioresistant (soft tissue sarcoma, melanoma, and rectal adenocarcinoma) and radiosensitive (renal cell carcinoma, head and neck squamous cell cancer, colon adenocarcinoma, and breast adenocarcinoma) histologies in the clinical correlation cohort.

Table 1:

Clinical characteristics of radioresistant and radiosensitive lung metastases

	Radioresistant	Radiosensitive	p-value
Patients (n)	53	52	
Lesions (n)	71	66	
Follow-Up, months (range)	15(1.2–73.3)	16.5(1.6–88.9)	
Age, years (range)	69(21–88)	66 (33–93)	0.14
Male/Female	29/24	36/16	0.13
Diameter of Lesion, cm, (range)	1.3(0.5–3.6)	1.5(0.3–4.4)	0.2
Dose 50 Gy/5, 60 Gy/5, 60 Gy/8	5/59/7	10/53/3	0.18
Lines of Previous Systemic Therapy (range)	1 (0–4)	1 (0–4)	0.97

Table 2:

Characteristics of Lesions Undergoing Local Failure

Lesion	Histology	Age	Maximum Size (cm)	Location	Dose	Time to Local Failure (Months)
Lesion 1	Sarcoma	65	1.1	RML	60 Gy/5	4.1
Lesion 2	Sarcoma	51	3.6	LLL	50 Gy/5	7.5
Lesion 3	Rectal	77	1.3	LUL	60 Gy/5	8.2
Lesion 4	Rectal	65	1.5	RUL	60 Gy/8	8.6
Lesion 5	Melanoma	30	0.6	RML	60 Gy/5	20.1

*RUL= Right upper lobe;

**RML=Right middle lobe;

***LUL = Left upper lobe;

****LLL = Left lower lobe